Electronic Supplementary Material (ESI) for Chemical Science.
This journal is © The Royal Society of Chemistry 2016

Supplementary Information

Highly specific noninvasive photoacoustic and positron emission tomography of brain plaque with functionalized croconium dye labeled by a radiotracer

Yajing Liu[a], Yanping Yang[b], Mingjian Sun[c], Mengchao Cui[b], Ying Fu[c], Yu Lin[a], Zijing Li*[a], and Liming Nie*[a]

[a]State Key Laboratory of Molecular Vaccinology and Molecular Diagnosis & Center for Molecular Imaging and Translational Medicine, School of Public Health, Xiamen University, Xiamen 361102, People's Republic of China

[b]Key Laboratory of Radiopharmaceuticals, Ministry of Education, College of Chemistry, Beijing Normal University, Beijing 100875, China.

[c]Department of Control Science and Engineering, Harbin Institute of Technology, 92 West Dazhi Street, Nan Gang District, Harbin 150001, China.

*Corresponding Authors: zijing.li@xmu.edu.cn; nielm@xmu.edu.cn.

Table of Content

Experimental section

Regents and Methods:

All chemicals employed in the synthesis were obtained commercially and used as received. 1-ethyl-3-(3-dimethyl aminopropyl) carbodiimide (EDC) and N-hydroxylsuccinimide (NHS) were purchased from J&K Chemical Ltd. Thioflavine S was obtained from Sigma-Aldrich. The ^{1}H NMR and ^{13}C NMR spectra were obtained at 600 MHz on an Avance II spectrometer (Bruker) in either DMSO-d_6 or $CDCl_3$ solutions at room temperature (r.t.) with tetramethylsilane (TMS) as an internal standard. Mass spectra (MS) and high-resolution mass spectra (HRMS) were acquired from an Equire 3000 plus system (Bruker) equipped with electrospray ionization (ESI) or a Q Exactive LC-MS/MS instrument (Thermo Fisher), respectively.

HPLC was performed on a Dionex Ulti-Mate 3000 system (Thermo Fisher) with a SPD-20A UV detector (λ = 254 nm, 800 nm). HYPERSIL GOLD C18 columns (Thermo Scientific, 5 μm, 4.6 mm × 250 mm and 10 mm × 250 mm) were used for HPLC analysis and separation respectively. The purity of the standard compound was determined by analytical HPLC (λ = 254 nm) and was higher than 96%. Fluorescence was observed with a FV1200 confocal microscope (Olympus, Japan). PA images were captured with a Nexus 128 system (Endra, USA). The microPET/CT scan was performed using an Inveon microPET-CT (Siemens, Germany). The distribution of CDA was detected by an IVIS Lumina II imaging system (Caliper Life Sciences, USA). AD models were induced with the five time familial AD (5×FAD) transgenic mice that coexpress a total of five FAD mutations [APP K670N/M671L (Swedish) + I716V (Florida) + V717I (London) and PS1 M146L + L286V].[1, 2] All animal studies were conducted in compliance with the animal care and use guidance established by Xiamen University animal care committee.

Synthesis:

*(Z)-2-(4-(Bis(2-hydroxyethyl)amino)-2-hydroxyphenyl)-4-(4-(bis(2-hydroxyethyl)iminio)-2-hydroxycyclohexa-2,5-dien-1-ylidene)-3-oxocyclobut-1-en-1-olate (**3**, SDA-1)：* Compound **2** was obtained following the previous literature.[3] Compound **3** was then prepared by refluxing the mixture of squaric acid (11.4 mg, 0.1 mmol) and compound **2** (39.4 mg, 0.2 mmol) in n-butanol and toluene (1:1, v/v, 3 mL) until no more precipitation. After cooling to r.t., the crude product was collected by filtration, washed with methanol and dried under vacuum to obtain the corresponding product as a very dark blue solid (41.5 mg, 88%). ^{1}H NMR (600 MHz, DMSO-d_6) δ: 11.79 (s, 2H), 7.69 (d, 2H, J = 7.8 Hz), 6.64 (dd, 2H, J = 9.6 Hz, J = 2.4 Hz), 6.25 (d, 2H, J = 2.4 Hz), 4.9 (s, 4H), 3.65-3.58 (m,16H).

(Z)-4-(5-(4-Carboxypiperidin-1-ium-1-ylidene)thiophen-2(5H)-ylidene)-2-(5-(4-carboxypiperidin-1-yl)thiophen-2-yl)-3-oxocyclobut-1-en-1-olate (7, SDA-2): The synthesis of compound **6** was performed following the previous literature.[4] Compound **7** was prepared by refluxing the mixture of squaric acid (11.4 mg, 0.1 mmol) and compound **6** (42.2 mg, 0.2 mmol) in n-butanol and toluene (1:1, v/v, 3 mL). The dark blue solid was obtained (41.5 mg, 83%). ^{1}H NMR (600 MHz, DMSO-d_6) δ: 7.77 (d, 2H, J = 4.8 Hz), 6.75 (d, 2H, J = 4.8 Hz), 2.62-2.61 (m, 2H), 2.01-1.98 (m, 4H), 1.70-1.66 (m, 4H).

*(Z)-2-(4-(Bis(2-hydroxyethyl)amino)-2-hydroxyphenyl)-5-(4-(bis(2-hydroxyethyl)iminio)-2-hydroxycyclohexa-2,5-dien-1-ylidene)-3,4-dioxocyclopent-1-en-1-olate (**8**, CDA-1):* Compound **8** was prepared by refluxing the mixture of croconic acid (0.1 mmol, 14.2 mg) and 3-N,N-dialkylaminophenol (0.2 mmol, 39.4 mg) in n-butanol and toluene (1:1, v/v, 3 mL). The product was obtained as a black solid (45 mg, 90%). Mass spectrum (ESI+), calculated for $C_{25}H_{28}N_2NaO_9^+$, m/z 523.17, found 523.17. ^{1}H NMR (600 MHz, DMSO-d_6) δ: 14.48 (s, 2 H), 8.82 (d, 2H, J = 12 Hz), 6.81-6.77 (m, 2H), 6.275 (d, 2H, J = 18 Hz), 3.71 (t, 12H, J = 24 Hz), 3.64 (t, 8H, J = 12 Hz). ^{13}C NMR (150 MHz, DMSO-d_6) δ: 188, 166, 158, 139, 134, 116, 112, 101, 59, 54.

*(Z)-5-(5-(4-Carboxypiperidin-1-ium-1-ylidene)thiophen-2(5H)-ylidene)-2-(5-(4-carboxypiperidin-1-yl)thiophen-2-yl)-3,4-dioxocyclopent-1-en-1-olate (**9**, CDA-2):*

Compound **9** was prepared following the previous literature, and a black solid was obtained (5.32 g, 95%).[4] HRMS (ESI-), calculated for $C_{25}H_{23}N_2O_7S^{2-}$, m/z 527.0952, found 527.0952. ^{1}H NMR (600 MHz, DMSO-d_6) δ: 12.46 (s, 2H), 8.51 (s, 2H), 7.05 (s, 2H), 4.01-4.04 (m, 4H), 3.50-3.56 (t, 4H, J = 18 Hz), 2.65-2.70 (m, 4H), 1.99-2.06 (m, 4H), 1.67-1.77 (m, 4H).

*(Z)-2-(5-(4-Carboxypiperidin-1-yl)thiophen-2-yl)-3,4-dioxo-5-(5-(4-((2-(tosyloxy)ethoxy)carbonyl)piperidin-1-ium-1-ylidene)thiophen-2(5H)-ylidene)cyclopent-1-en-1-olate (**10**):* A solution of tosyl chloride (4 g, 21 mmol) in tetrahydrofuran (20 mL) was added slowly over 1 h to the solution of ethylene glycol (0.21 mol) and triethylamine (2.5 g, 25 mmol) in tetrahydrofuran (200 mL) at 0 ℃. The mixture was stirred for 6 hours and then extracted with water and ethyl acetate. The organic layer was dried over anhydrous Na_2SO_4 and concentrated in reduce pressure rotary evaporator to give 2-hydroxyethyl 4-methylbenzenesulfonate (see **Scheme S2**). It was purified by silica gel column chromatography using petroleum ether and ethyl acetate as eluent. Into a 50 mL round-bottomed flask, compound **9** (50 mg, 0.09 mmol), DMAP (2.3 mg, 0.02 mmol), EDCI (43.56 mg, 0.23 mmol), and N,N-Dimethylformamide (1 mL) were charged. A solution of 2-hydroxyethyl 4-methylbenzenesulfonate (20.46 mg, 0.09 mmol) in N,N-Dimethylformamide (0.5 mL) was then added drop by drop. The mixture was stirred at r.t. for 24 h and then purified by silica gel column chromatography. Compound **10** was obtained as a black solid, yield 86%.

*(Z)-2-(5-(4-Carboxypiperidin-1-yl)thiophen-2-yl)-5-(5-(4-((2-fluoroethoxy)carbonyl)piperidin-1-ium-1-ylidene)thiophen-2(5H)-ylidene)-3,4-dioxocyclopent-1-en-1-olate (**11**, CDA-3):* Into a 5 mL vial, compound **9** (50 mg, 0.09 mmol), DMAP (2.3 mg, 0.02 mmol), EDCI (43.56 mg, 0.23 mmol), and N,N-Dimethylformamide (1 mL) were charged. A solution of 2-fluoroethanol (6.06 mg, 0.09 mmol) in N,N-

Dimethylformamide (0.5 mL) was then added drop by drop. The mixture was stirred at r.t. for 24 h and then purified by silica gel column chromatography. A black precipitate (compound **11**) was obtained with a yield of 91%. ^{1}H NMR (600 MHz, DMSO-d_6) δ: 12.5 (s,1H), 8.5 (s, 2H), 7.04 (d, 2H, J = 3.9 Hz), 4.44 (t, 1H, J = 4.3 Hz), 4.35 (t, 3H, J = 4.3 Hz), 4.00 (d, 4H, J = 6.7 Hz), 3.63 (t, 1H, J = 4.3 Hz), 3.57 (t, 1H, J = 3.5 Hz), 3.52 (t, 4H, J = 11.4 Hz), 2.68-2.65 (m, 2H), 2.04 (q, 4H, J_1 = 13.4 Hz, J_2 = 2.8 Hz), 1.76-1.71 (m, 4H). ^{13}C NMR (150 MHz, DMSO-d_6) δ: 182.05, 175.48, 122.95, 115.03, 86.30, 85.20, 60.89, 60.76, 51.16, 27.96. ^{19}F NMR (564 MHz, DMSO-d_6) δ: -222.5.

Radiochemistry:

[^{18}F]CDA-3: A QMA Light cartridge (Waters, USA) was activated and dried by airflow. [^{18}F]fluoride was trapped on the cartridge and then eluted with 1.0 mL of Kryptofix$_{222}$/K_2CO_3 solution (13.0 mg of Kryptofix$_{222}$ and 1.1 mg of K_2CO_3 in CH_3CN/H_2O, 4 : 1, v:v). To remove H_2O, the sample was heated at 120 ˚C under a stream of nitrogen gas. The residue was then azeotropically dried with 300 μL anhydrous acetonitrile three times at 120 ˚C under a stream of nitrogen gas. For [^{18}F]CDA-3 labeling, 0.5 mg precursor **10** was dissolved in 1.0 mL anhydrous acetonitrile and mixed with the dried $^{18}F^-$ (37 MBq) before 5 min heating at 90 ℃. The mixture was cooled to r.t. before purification by HPLC (Thermo Scientific, USA). HPLC condition: a HYPERSIL GOLD C18 column, 5 μm, 10 mm × 250 mm, CH_3CN/H_2O = 65/35; flow rate = 4.0 mL/min. The retention time of [^{18}F]CDA-3 was 18.6 min in this HPLC system and the total radiochemical yield was 31±3% (decay not corrected, at the end of synthesis). The preparation took approximately 30 min and the radiochemical purity was greater than 96%.

***In vitro* binding potency towards A*β* peptide aggregates (A$\beta_{1\text{-}40}$) across molecular docking:**

CDA-3 was firstly constructed with GaussView 5.0. Geometric optimizations were performed in Gaussian 09 (Gaussian 09, Revision C.01, Gaussian, Inc., Wallingford CT, 2010) using B3LYP/6-31G in the water phase. A lamarckian genetic algorithm was used to perform docking simulations on Aβ fibers (PDB ID: 2LMN) with AutoDock4.0 according to previously described methods.[5-8] For the docking simulations, the C-N bonds of the ligand were kept rotatable. The size of the grid was chosen to occupy the whole peptide molecule (96 × 62 × 72 Å^3 dimensions with a grid spacing of 0.836 Å). Each docking trial produced 100 poses.

The binding energy of CDA-3 was measured according to previously reported procedures.[7] Molecular docking was performed using AutoDock4.0. The AutoDock semi-empirical force field was used to predict the binding energy.

The acute lethal dose (LD_{50}) study

Forty Kunming mice were divided into five groups depending on different dose (n=8). Before CDA-3 treatment, these mice were fasted and had access to water. At each dose, mice were intravenously injected with CDA-3 solutions (0.2 mL/20 g body weight) and observed for 24 h. Symptoms and mortalities of each group were recorded.

Fluorescence imaging *in vitro* and *in vivo*:

To assess the maximal imaging depth of the CDA probe, CDA (0.04 mg/mL) in tubes were covered with different thicknesses of brain and followed by fluorescence imaging (excitation wavelength = 760 nm, emission wavelength = 830 nm). The fluorescent intensities were taken using Carestream FX Pro imaging system. The accumulation of CDA in 5×FAD mice was then examined by fluorescent imaging. All mice were anesthetized with isoflurane and intravenously injected with CDA dye (100 μL, 1 mg/mL). After intravenously administration, the mice were received fluorescence imaging and recorded by CCD camera.

In vitro* evaluation via fluorescence staining studies on 5×FAD transgenic mouse brain tissue:*

After *in vivo* imaging studies was completed, the animals were perfused with saline solution. Brains of 5×FAD and littermate mice were removed and fixed immediately in 4% paraformaldehyde. 10-μm-thick brain sections were cut coronally with a sliding microtome. The adjacent sections were prepared to detect amyloid deposits. The localization of Aβ plaques was confirmed by labeling brain with CDA and thioflavin-S (Th-S) on the adjacent sections. One set of fixed sections was immersed in 0.125% Th-S solution for 3 min and the other set of sections was stained with fresh CDA. Finally, brain sections were washed with 40% EtOH and 0.2 M PBS (pH = 7.4) for 10 min. The Th-S and CDA-positive amyloid plaques were visualized with a FV1200 fluorescent microscope (Olympus) equipped with filters for GFP (excitation = 488 nm; emission = 520 nm).

***In vivo* PAT study**:

PA images of CDA dye were evaluated using a hemispherical PAT system. It consists of a NIR laser, 128 ultrasonic transducers, and reconstruction system. Owing to the built-in hemispherical configuration, the PA system can collect signals from multiple angles. PAT was conducted at 800 nm with pulse energy of 1.5 mJ/cm^2. Filtered back-projection reconstruction algorithm was used to reconstruct PA images. Anesthetized mice (5×FAD and littermate wild-type mice, 3-4 months old) were depilated and laid on the animal tray, which was placed inside the imaging bowl filled with deionized water to allow acoustic coupling. Following the intravenous injection of CDA, PA monitoring was performed over 8 hours.

In vivo* microPET-CT imaging:*

The microPET-CT imaging was further performed in live transgenic mice and age-matched wild-type mice. After i.v. injection of ~1.85 MBq of [^{18}F]CDA-3 (100 μL), mice were anesthetized immediately prior to the PET scan with isoflurane (2.5%) in 75% N_2 plus 22% O_2 for 3–5 min. For maintenance of anesthesia during the scan the isoflurane was reduced to 1-1.5%. The imaging data were acquired using a multimodality Inveon microPET-CT system (Siemens, Germany). A baseline low-dose CT scan was then obtained for localization and attenuation correction. The images were reconstructed by a 3D OPMAP reconstruction algorithm from the Inveon Acquisition Workplace Software (Siemens, Germany).

Supplementary Figures

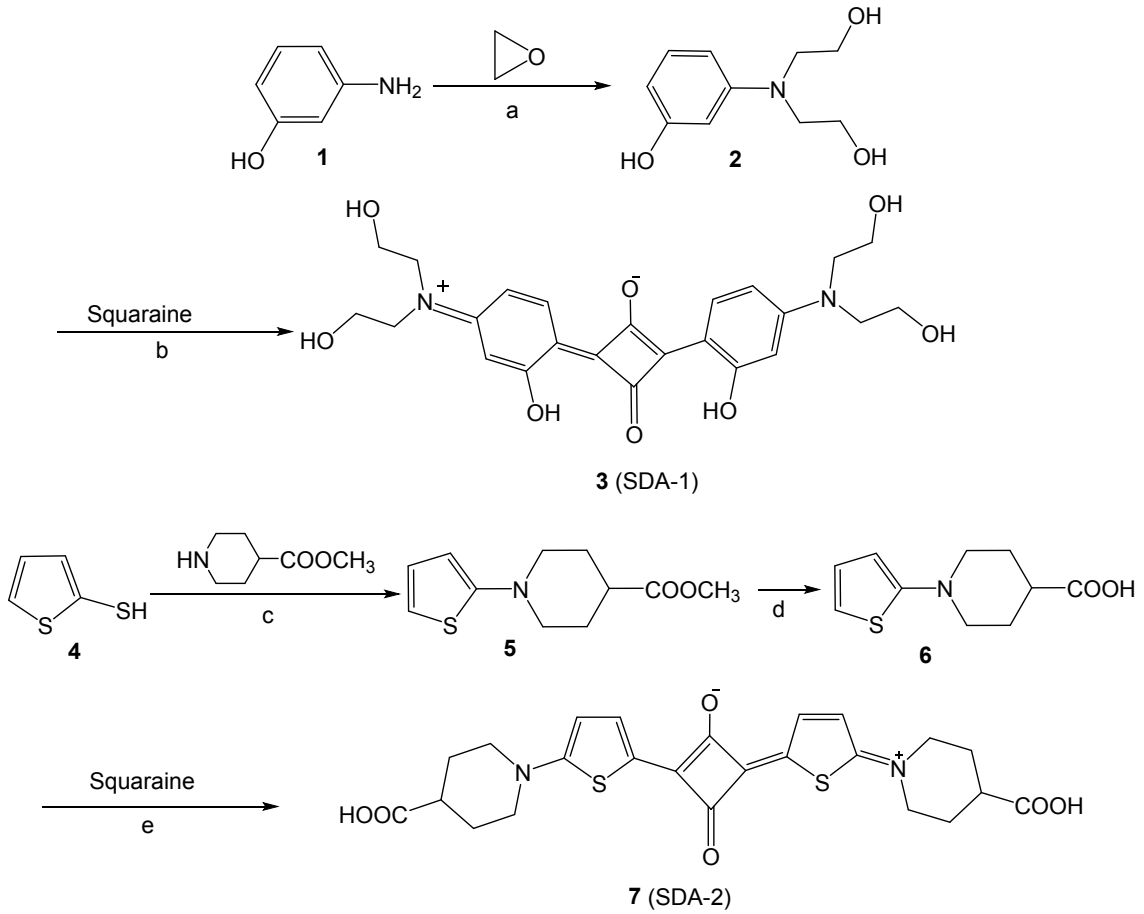

Scheme S1[a]. Synthetic routes of SDA-1, SDA-2. [a]Regents and conditions: (a) Toluene, reflux, 1h; (b) (I) Toluene/1-butanol, reflux, 1 h; (II) $NaHCO_3$, H_2O; (c) THF, K_2CO_3; (d) (I) NaOH, H_2O; (II) HOAc; (e) Toluene/1-butanol, reflux, 1 h.

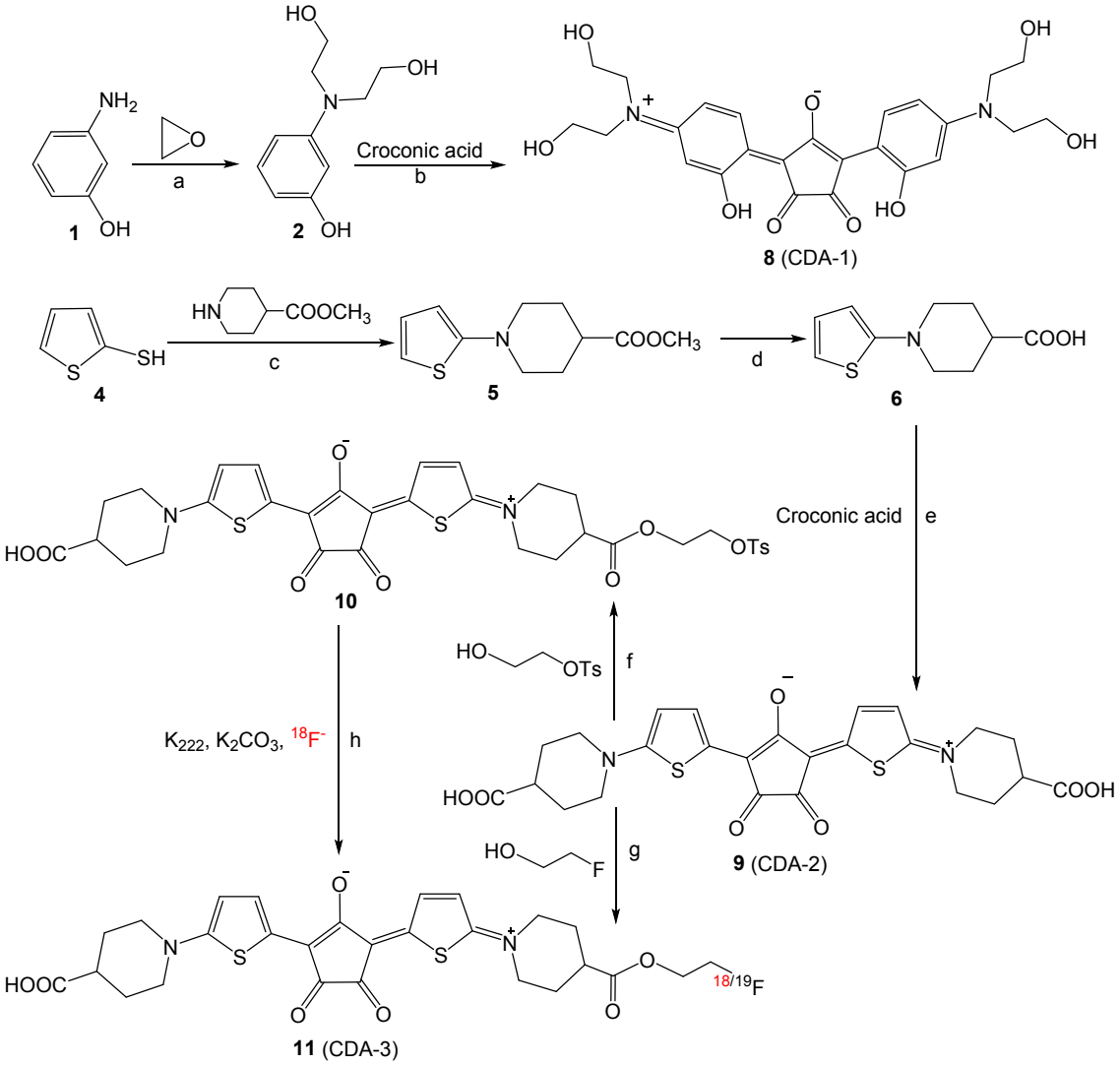

Scheme S2 [a]. Synthetic routes of CDA-1, CDA-2, and CDA-3. [a]Regents and conditions: (a) Toluene, reflux, 1h. (b) (I) Toluene/1-butanol, reflux, 1 h; (II) $NaHCO_3$, H_2O. (c) THF, K_2CO_3. (d) (I) NaOH, H_2O; (II) HOAc. (e) Toluene/1-butanol, reflux, 1 h. (f) DMAP, EDCI, N,N-Dimethylformamide, 24h. (g) DMAP, EDCI, N,N-Dimethylformamide, 24h. (h) CH_3CN, 5 min, 120 ˚C

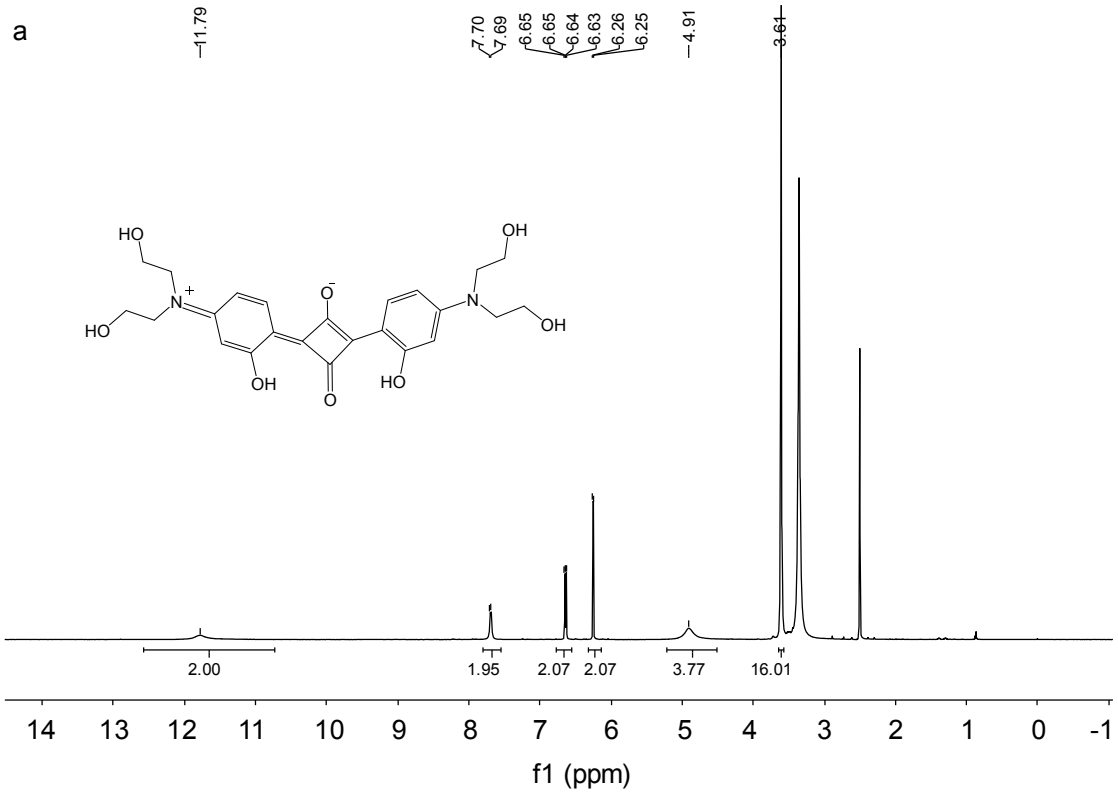

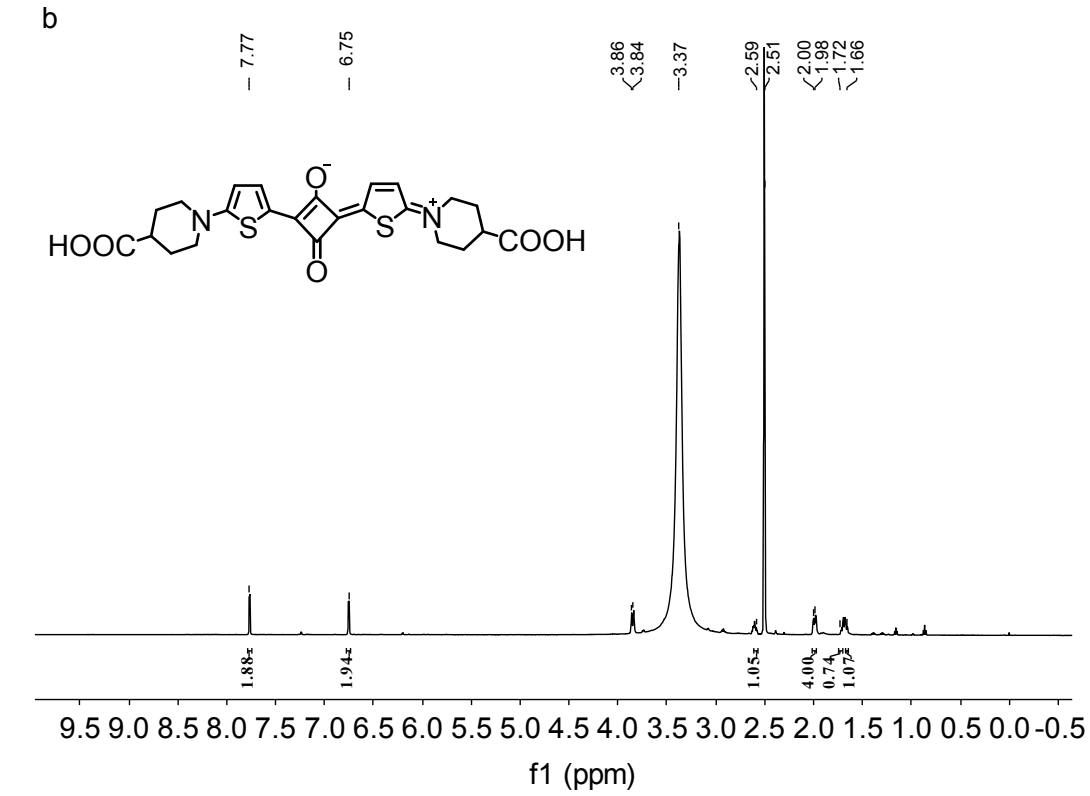

Figure S1 ^{1}H NMR of (a) SDA-1 and (b) SDA-2.

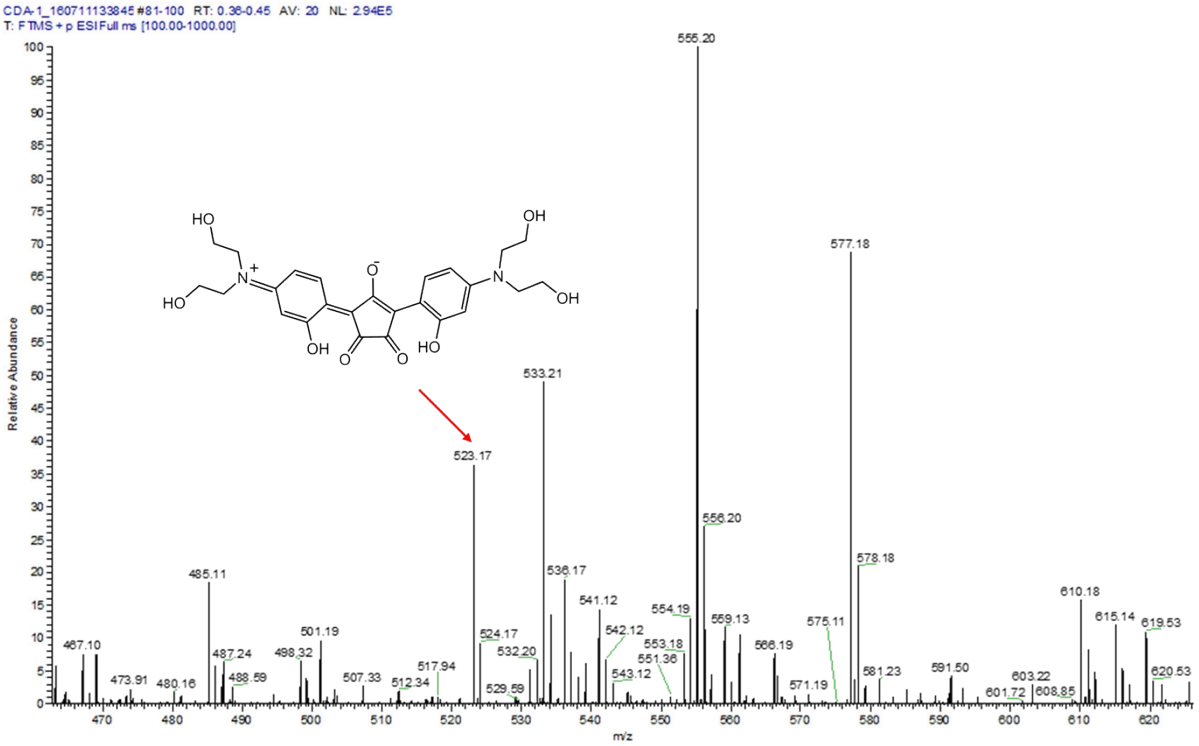

Figure S2 Mass spectrum of CDA-1.

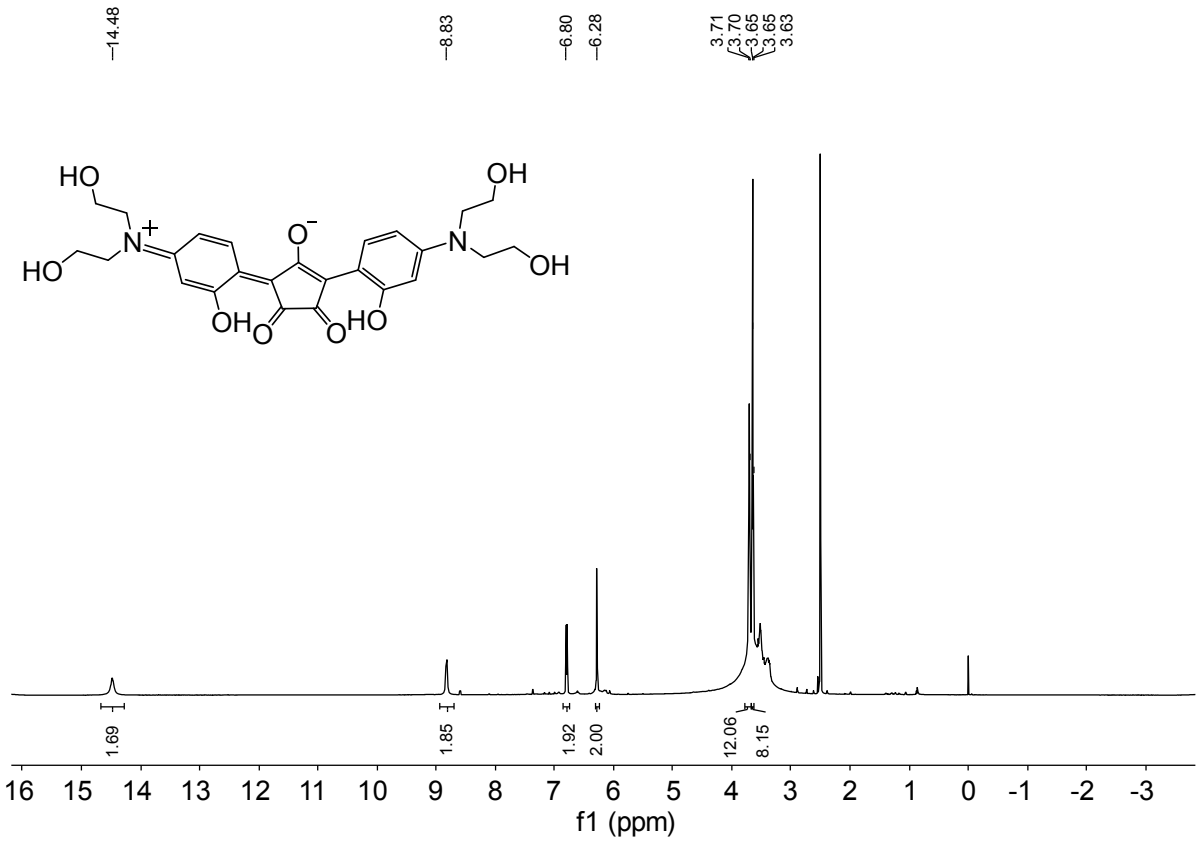

Figure S3 ^{1}H NMR of CDA-1.

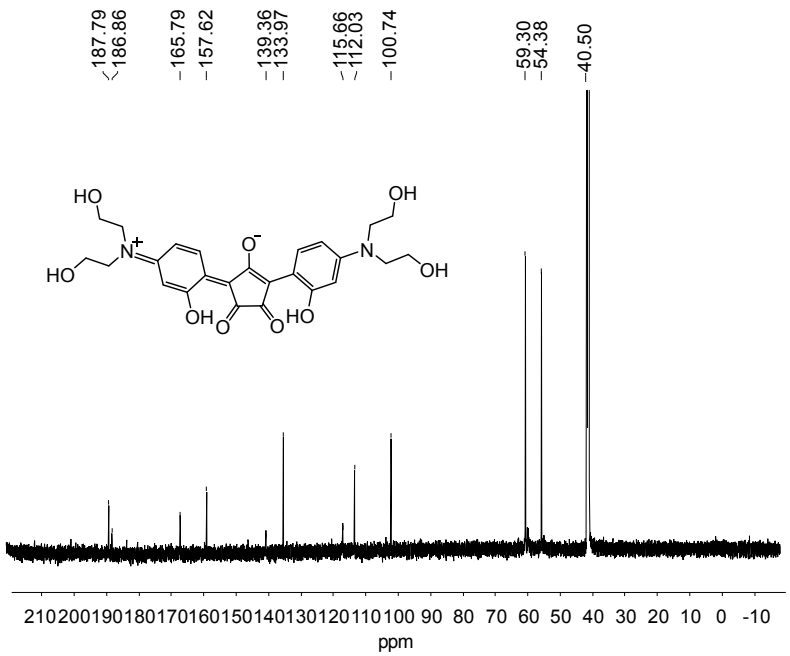

Figure S4 ^{13}C NMR of CDA-1.

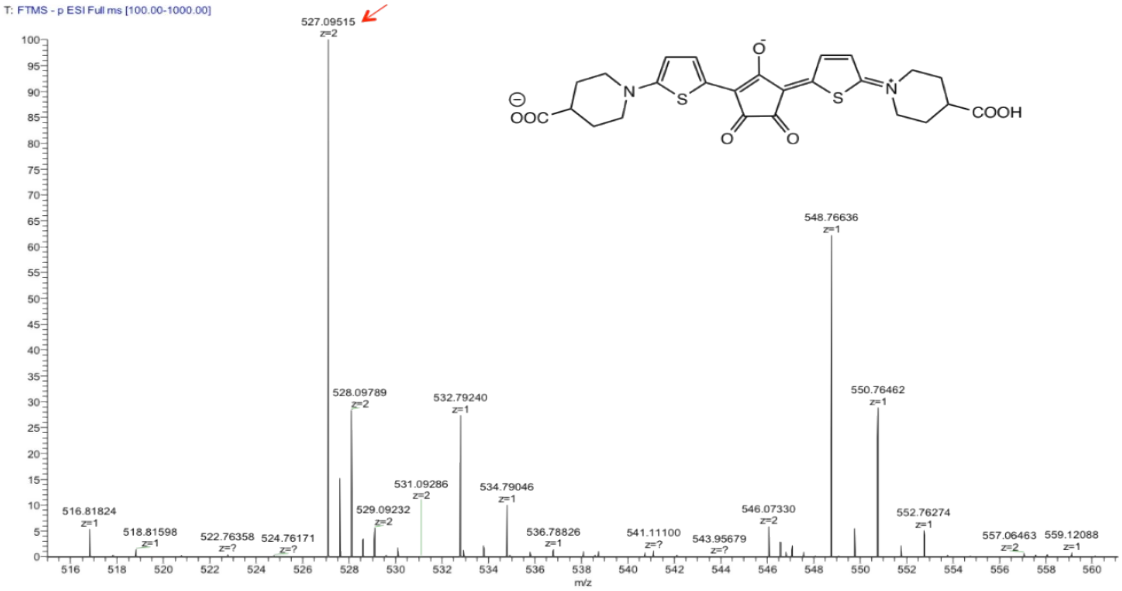

Figure S5 HRMS of CDA-2.

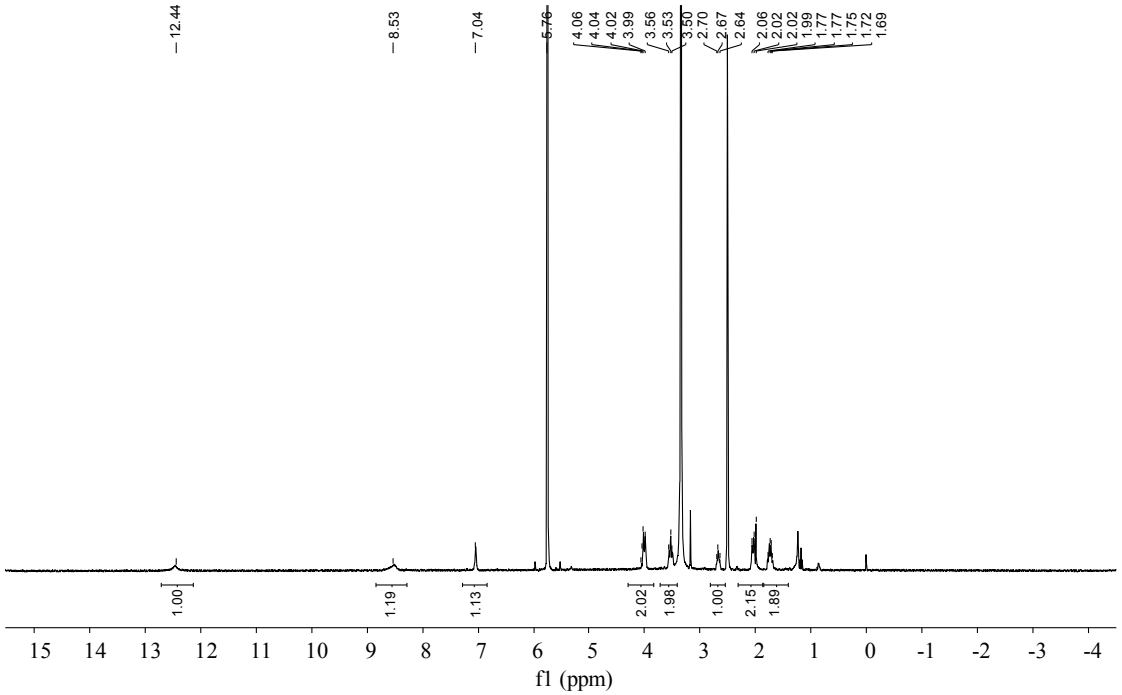

Figure S6 ^{1}H NMR of CDA-2.

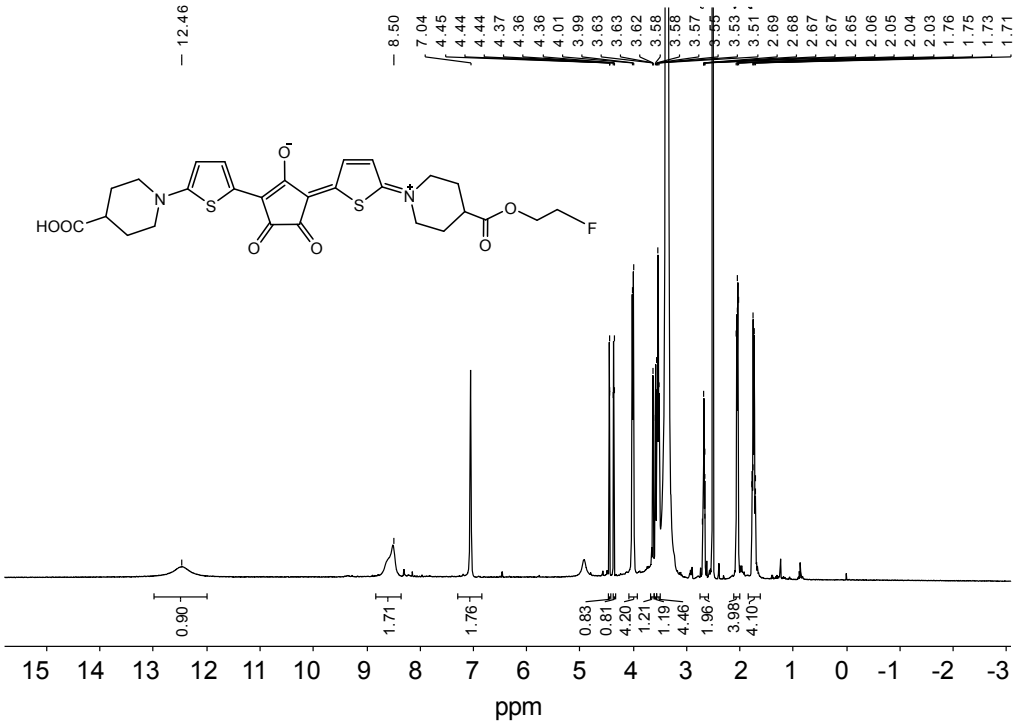

Figure S7 ^{1}H NMR of CDA-3.

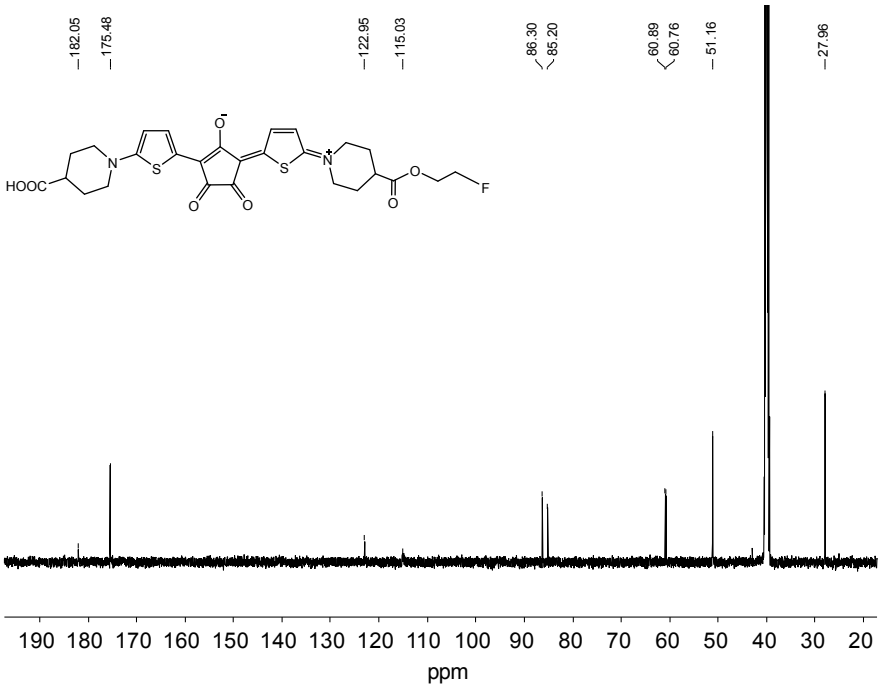

Figure S8 ^{13}C NMRof CDA-3.

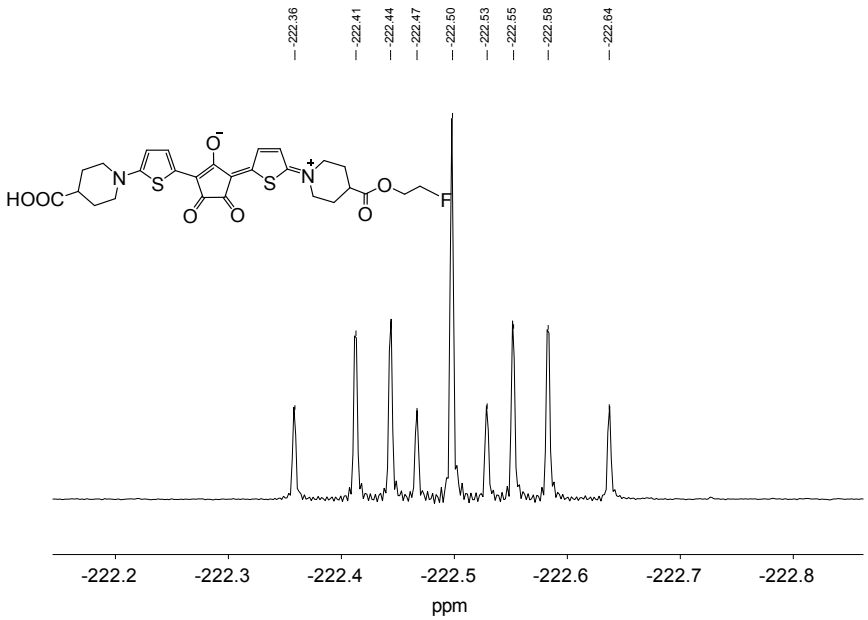

Figure S9. ^{19}F NMR of CDA-3.

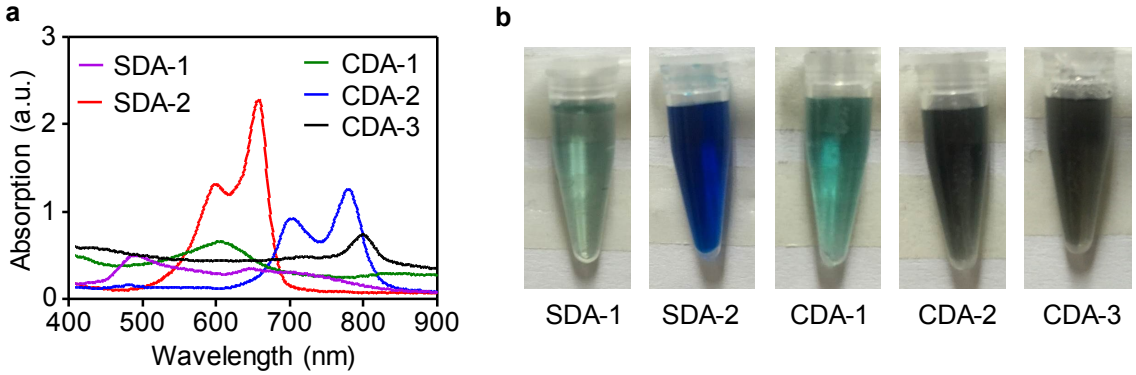

Figure S10 (a) Absorption spectra recorded for SDA-1, SDA-2, CDA-1, CDA-2, and CDA-3 in water. (b) Corresponding photographs of SDA-1, SDA-2, CDA-1, CDA-2, and CDA-3.

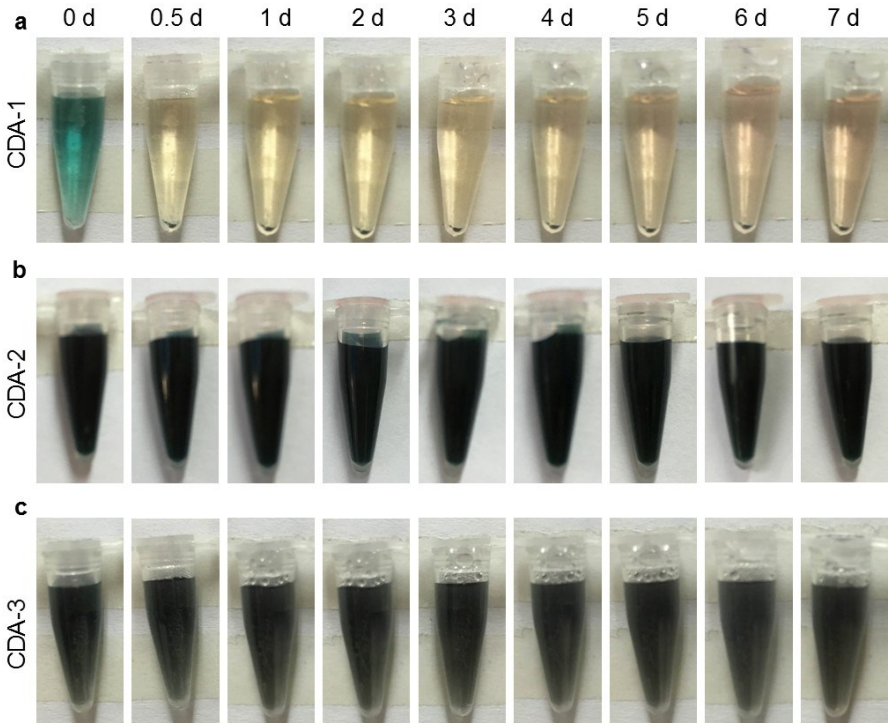

Figure S11 The stability of CDA-1,CDA-2, and CDA-3 in water at room temperature after 7 day storage.

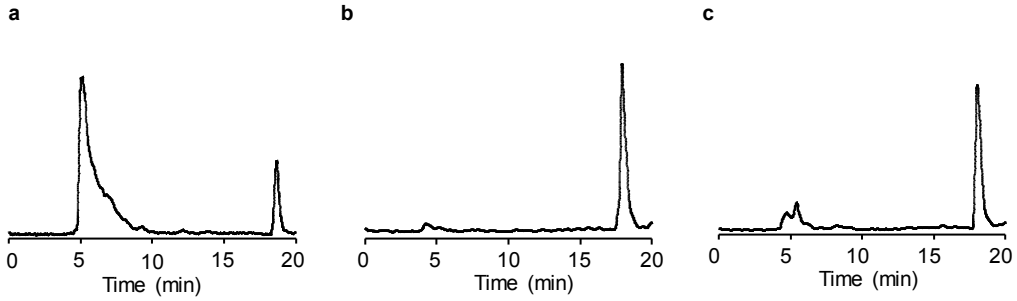

Figure S12 (a) The labeling rate and (b) purity of [^{18}F]CDA-3. (c) The stability of [^{18}F]CDA-3 was investigated after 2 h incubation.

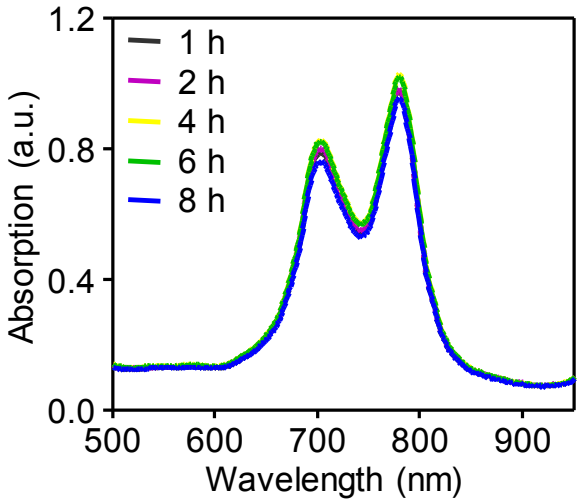

Figure S13 The absorption spectra of CDA-3 at different time points after incubation with human serum albumin.

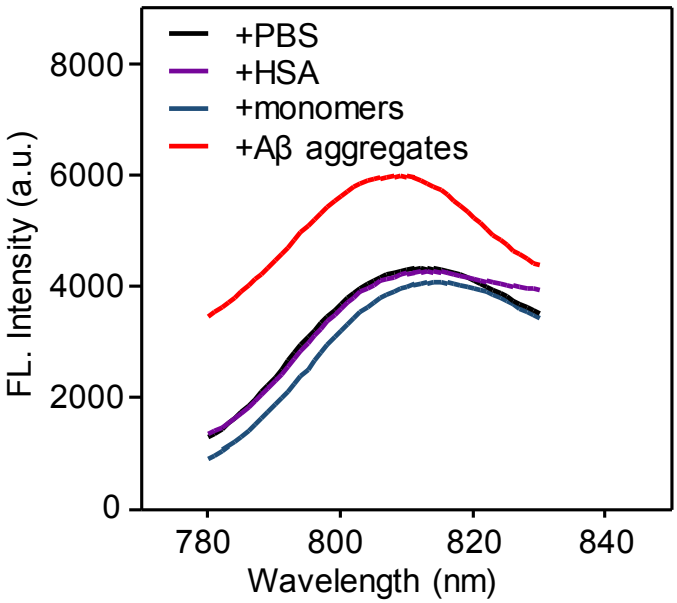

Figure S14 Fluorescence intensity of CDA-3 in PBS and in the presence of HSA, A$\beta_{1\text{-}40}$ monomers, and A$\beta_{1\text{-}40}$ aggregates.

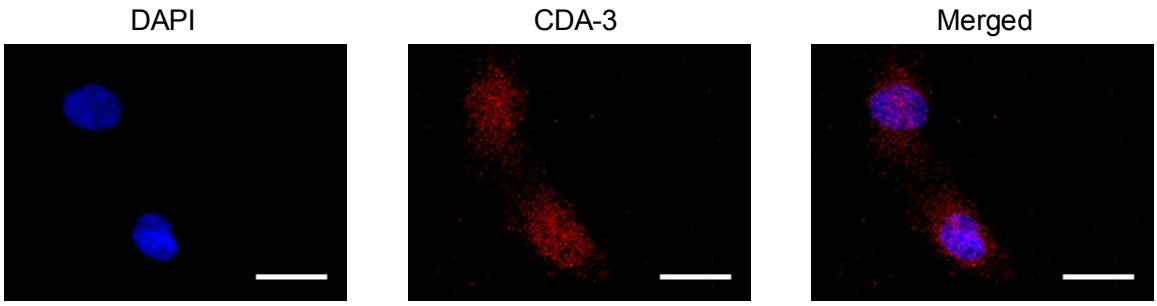

Figure S15 Fluorescent staining of human neuronal cell (SH-SY5Y) by CDA-3 and DAPI. Scale bar = 25 μm.

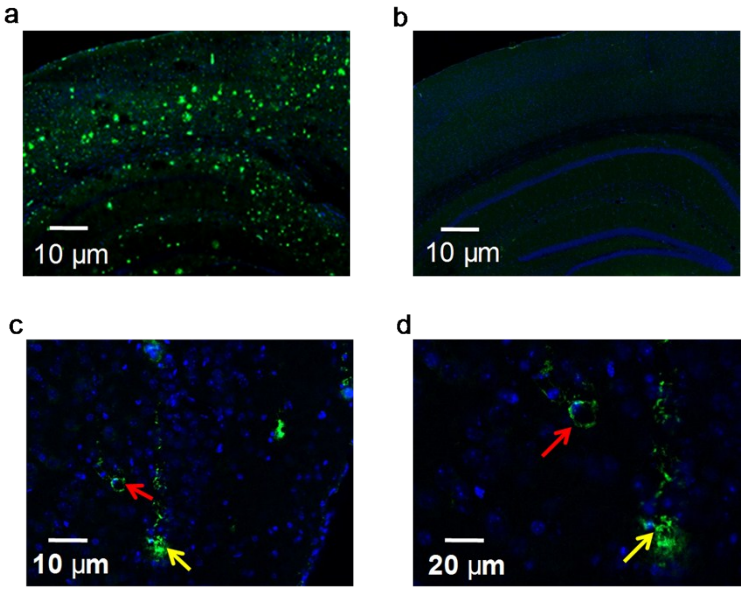

Figure S16 *In vitro* fluorescent staining of A*β* plaques by 6E10 and dapi on hippocampal section of (a) a Tg model mouse and (b) a WT mouse. (c) Cortex section staining of a Tg model mouse. (d) Amplification image of (c).

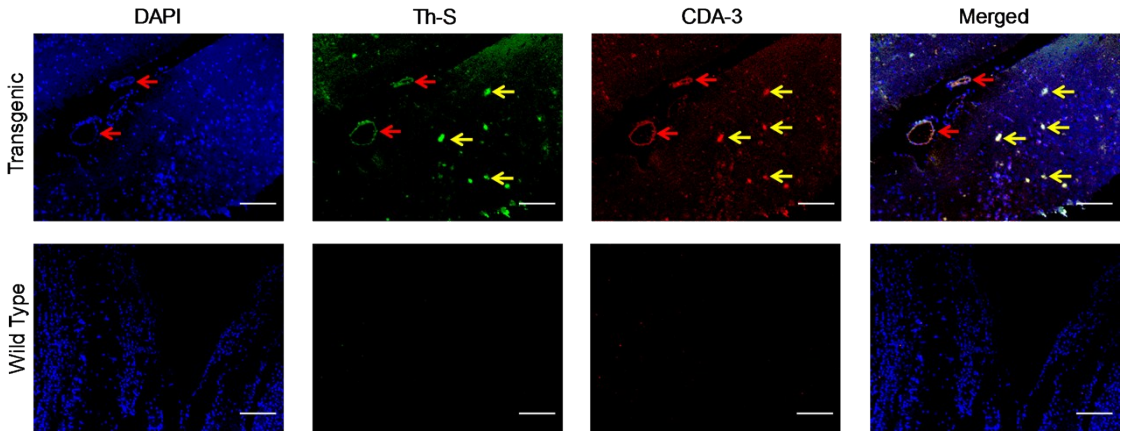

Figure S17 *In vitro* fluorescent staining of Aβ plaques by CDA on brain section of Tg and WT mice with filter set of Cy5.5. The presence and distribution of plaques on the sections were confirmed by fluorescence staining using Th-S on the same section with filter set for GFP. Scale bar = 100 μm.

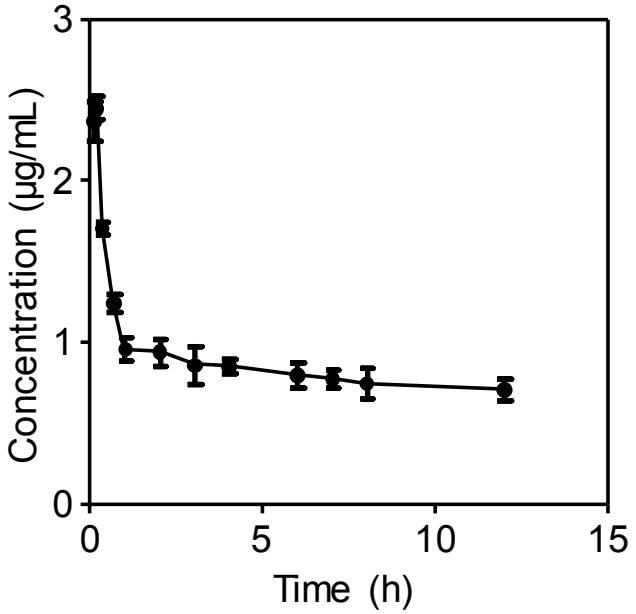

Figure S18 The concentration-time curve of CDA-3 in serum after intravenous injection.

References

1. M. Cacciottolo, A. Christensen, A. Moser, J. Liu, C. J. Pike, C. Smith, M. J. LaDu, P. M. Sullivan, T. E. Morgan, E. Dolzhenko, A. Charidimou, L. O. Wahlund, M. K. Wiberg, S. Shams, G. C. Chiang and C. E. Finch, *Neurobiology of aging*, 2016, **37**, 47-57.
2. S. Jawhar, A. Trawicka, C. Jenneckens, T. A. Bayer and O. Wirths, *Neurobiology of aging*, 2012, **33**, 196.e129-140.
3. C. Feau, E. Klein, C. Dosche, P. Kerth and L. Lebeau, *Organic & biomolecular chemistry*, 2009, **7**, 5259-5270.
4. S. Wang, T. Cong, Q. Liang, Z. Li and S. Xu, *Tetrahedron*, 2015, **71**, 5478-5483.
5. G. M. Morris, D. S. Goodsell, R. S. Halliday, R. Huey, W. E. Hart, R. K. Belew and A. J. Olson, *Journal of computational chemistry*, 1998, **19**, 1639-1662.
6. G. M. Morris, R. Huey, W. Lindstrom, M. F. Sanner, R. K. Belew, D. S. Goodsell and A. J. Olson, *Journal of computational chemistry*, 2009, **30**, 2785-2791.
7. R. Huey, G. M. Morris, A. J. Olson and D. S. Goodsell, *Journal of computational chemistry*, 2007, **28**, 1145-1152.
8. R. Huey, D. S. Goodsell, G. M. Morris and A. J. Olson, *Letters in Drug Design & Discovery*, 2004, **1**, 178-183.